Mechanisms of spike inhibition in a cortical network induced by transcranial magnetic stimulation

Yoichi Miyawaki [a,1] Masato Okada [a,b]

[a] *RIKEN Brain Science Institute, 2-1, Hirosawa, Wako, Saitama 351-0198, JAPAN*

[b] *"Intelligent Cooperation and Control", PRESTO, JST, c/o RIKEN Brain Science Institute, 2-1, Hirosawa, Wako, Saitama 351-0198, JAPAN*

Abstract

We propose mechanisms of neural interference induced by transcranial magnetic stimulation (TMS). TMS is widely used as a powerful and unique experimental tool to stimulate the human brain noinvasively, which typically induces inhibitory effect on the cortical functions. However, the fundamental mechanism of TMS-induced suppression is still unclear. In this paper, we computationally demonstrate that TMS induces sustained spike inhibition in a conductance-based network model without the ion channel which is necessary for spike inhibition in an isolated single neuron, suggesting that each individual neuron is not necessarily suppressed by TMS; rather, a collapse of excitatory and inhibitory input balance in the cortical network is crucial for TMS-induced suppression.

Key words: TMS; Spike inhibition; Conductance-based model; Perturbation; AHP channel

1 Introduction

Transcranial magnetic stmiulation (TMS) is an experimental tool to stimulate the human brain noninvasively with high temporal resolution through a brief magnetic pulse yielded by a coil placed on the scalp. TMS typically causes inhibitory effect on the cortical functions; e.g. a part of visual field can be

[1] Corresponding author, E-mail address: yoichi_miyawaki@brain.riken.jp

erased by the occipital stimulation [1], and peripheral electromyogram can be suppressed by the mortor cortical stimulation [2]. These striking results have appealed to various applications in cognitive neuroscience fields. However, the neural mechanisms of TMS-induced effect is still unknown though twenty years have passed since the first cortical stimulation was successfully made [3].

We computationally approach this question using a conductance-based network model. A few past studies discussed the spike generation or inhibition process induced by a brief magnetic pulse applied to an isolated single neuron [4][5], in which they suggested that afterhyperpolarization (AHP) channel plays a critical role in TMS-induced spike inhibition in a single neuron level [5]. On the other hand, our previous studies demonstrated that the simplest one-population rate network model without any spike adaptation mechanisms could be inhibited by the TMS-like perturbation uniformly given to all the neurons, and the temporal properties of the suppression were totally consistent with various experimental data [6][7]. This fact suggests that TMS-induced suppression might be mediated by inhibitory interaction in the cortical network rather than a particular membrane mechanism in a single neuron level. In this paper, we use a conductance-based network model, in which each neuron has Hodgkin-Huxley type ion channel mechanisms but excludes AHP channel. We analyze TMS effect on the spiking network and elucidate the critical mechanisms for spike inhibition induced by TMS.

2 Model

We used a single compartment model as an individual neuron,

$$C_m \frac{dV_i(t)}{dt} = g_i^{\text{leak}}(E_i^{\text{leak}} - V_i(t)) - I_i^{\text{ion}}(t) + I_i^{\text{syn}}(t) \tag{1}$$

where I_i^{ion} is the active ion current of the i-th neuron including the fast sodium, delayed rectifier, and A-type current. Each ion current obeys Hodgkin-Huxley type kinetics. I_i^{syn} is the synaptic input current given from the other neurons inside the network and the afferent terminal,

$$I_i^{\text{syn}}(t) = \sum_{j=1}^{N} g_{ij}^{\text{net}}(t)(E_j - V_i(t)) + g_i^{\text{ext}}(E^{\text{ext}} - V_i(t)) \tag{2}$$

$$g_{ij}^{\text{net}} = -J_0 + J_2(1 + \cos(2(\theta_i - \theta_j))) \qquad (\theta_i = -\frac{\pi}{2} + i\frac{\pi}{N}) \tag{3}$$

$$\frac{dg^{\text{syn}}}{dt} = -\frac{g^{\text{syn}}}{\tau^{\text{syn}}} + G^{\text{syn}} \sum_{t_j} \delta(t - t_j). \tag{4}$$

The synaptic weight from neuron j to i, g_{ij}^{net}, consists of two parts: the uniform inhibition J_0 and the feature-specific interaction J_2, by which the network shows a local excitation around a given stimulus feature like orientation tuning function in the primary visual cortex. The firing rate of the afferent input was modeled as $f_{\text{ext}}(\theta_i - \theta_0) = \bar{F}(1 - \epsilon + \epsilon\cos(2(\theta_i - \theta_0)))$ to be weakly modulated according to difference between the prefered feature of a neuron and the stimulus feature θ_0. The synaptic decay was modeled by the 1st-order differential equation as Eq. 4.

We assumed that the TMS perturbation would be constant for all neurons in the local network because the spatial extent of the neural population is small compared with the spatial gradient of the induced electric field. Thus we simply added the TMS current, $I^{\text{TMS}}(t)$, on the right hand side of Eq. 1 as an external current input. Here we employ a simple rectangular pulse input with 1 ms duration (typical value of a commercially available system) as a TMS-like perturbation.

3 Results

Our previous studies suggest that the network needs to exhibit bistability to induce a sustained suppression by TMS. However, it is hard to search the proper network parameter for the bistable mode directly from the complicated conductance-based network model. Thus, we applied Shriki's method [8] to link the parameter space of the rate model to that of the conductance-based model. We firstly constructed the analog rate model which has the same synaptic structure as the conductance-based model, and fitted the output function of the rate model to the f-I curve of a single spiking neuron in the conductance-based model. Secondly, in the fitted rate model, we computed the phase boundary between monostable and bistable region regarding to excitatory and inhibitory synaptic weight, J_0 and J_2 (Fig. 1A). Finally, we remapped the parameter set of the bistable region back into the corresponding parameters for the conductance-based model. Using this method, we could make the complicated conductance-based model to be tractable, and we could easily find the proper parameter region in which the conductance-based model showed bistablity (Fig. 1B). In addition, we employed an afferent input model consisting of suprathreshold transient (mean rate: $\bar{F}^{\text{T}} > \bar{F}^{\text{T}}_{\text{thres}}$, duration: D^{T}) and subthreshold sustained (mean rate: $\bar{F}^{\text{S}} < \bar{F}^{\text{S}}_{\text{thres}}$) components. This is the simplest input model that leads the network into the bistable regime, yet it still captures the common properties of neural signals in brain areas such as the LGN and visual cortex.

Fig. 2A illustrates an example of a stable spiking pattern when the network was driven in the bistable regime. After the output firing frequency became

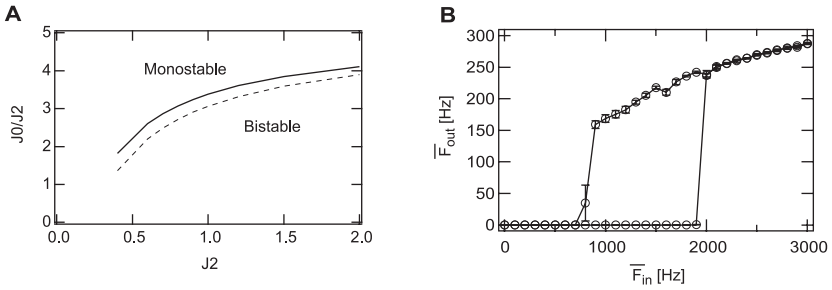

Fig. 1. A) Phase diagram of the rate model whose structure is the same as the conductance-based model noted in Sec. 2 (thick line: the boundary below which the network exhibits bistability. thin line: the boundary below which the network can hold the excitatory state even if the afferent input is terminated). B) An exmaple of bistability of the conductance-based model showing hysteresis for the afferent input intensity. The corresponding parameter set was remapped from the bistable regime in the phase diagram of the rate model.

stable, we applied the TMS-like perturbation to the network and could observe sustained spike inhibition (Fig. 2B). The minimum intensity of the perturbation was in the same order as the excitatory and inhibitory synaptic input current ($\sim 10^2 \mathrm{mS/cm^2}$). The reduction of the firing rate was slow (more than 50 ms at most), and such a slow relaxation was also clearly observed in the excitaroty and inhibitory input conductances (Fig. 2C). The balanced input given through the excitatory and inhibitory conductance was collapsed by the perturbation (Fig. 2C), and the network could not maintain the stable firing pattern and converged to the quiescent state. These basic properties of spike inhibition were consistenly observed regardless of the induction timing if it was applied in the steady state.

We also examined the effect of TMS on an isolated single neuron by using a multicompartment model with the reconstructed dendritic arborization [9]. The significant differences between our conductance-based model and this multicompartment model were calcium-related ion mechanisms: high-threshold Ca^{2+}, Ca^{2+}-dependent K^+ channel, and Ca^{2+} buffer and pump were included in the soma and dendrite in only the multicompartment model. We injected a constant somatic current and induced a specific spiking pattern depending on its morphology (Fig. 3B). Intracellular TMS current was calculated by the inner product of electric field direction of TMS and each neurite direction multiplied by the axial conductance (see detail in [5][7]). We could also observed spike inhibition for over 100 ms after a brief bursting period with Ca^{2+} rush-in and increase in $K^+_{(Ca^{2+})}$ (AHP channel) conductance. The minimum intensity of the suppressive perturbation was in the same order of somatic input current. However, this spike inhibition was observed in the very limitted condition. It was selective about cellular morphology; e.g., no spike inhibition was observed in layer IV stellate cell and more bushy layer V pyramidal cell. Even using the most susceptible morphology, it was hard to suppress the spike train if the current input was strong and the cell fired at high frequency more than

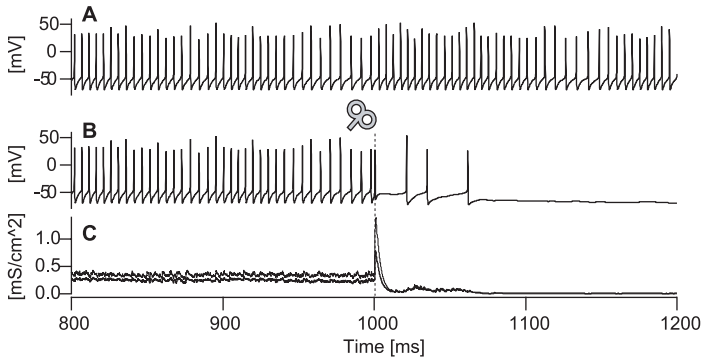

Fig. 2. A) The spiking pattern in the conductance based network model. This is an example of a single neuron whose selectivity is the same as the central point of the afferent input. B) Suppression of the spike train by the TMS-like perturbation. C) Excitatory (thick line) and inhibitory (thin line) input conductance. The parameters used here were $\bar{F^T} = 2800$ Hz, $D^T = 200$ ms, $\bar{F^S} = 1000$ Hz, $\theta_0 = 0$, $N = 100$, $J_0 = 0.021$ mS/cm^2, $J_2 = 0.008$ mS/cm^2, and other parameters were the same as [8].

about 40 Hz. In addition, duration of the spike inhibition strongly depends on the maximum conductance of $K^+_{(Ca^{2+})}$ channel. Under the condition that $K^+_{(Ca^{2+})}$ channel was completely blocked, no spike inhibition was observed by TMS of ten times intensity of the minimum suppressive value. On the other hand, the network model showed a stable spike inhibition by TMS in a wide range of firing frequency, even though $K^+_{(Ca^{2+})}$ channel was not included as a member of ion channel. We also successfully observed the sustained inhibitory effect by a subthreshold TMS, which results agree with experimental data of occipital TMS examining the relationship between phosphene threshold and the paired-pulse TMS interval [10].

4 Discussion

We constructed the conductance-based spiking network model having a cosine-type feature specific interaction as synaptic weights. If the network holds bistability, the TMS-like perturbation could stop the spike trains and the network finally converged to the quiescent state. These basic result was totally consistent with the prediction from the simple rate model's result [6][7]. The crucial point of the results is that the sustained spike inhibition was observed in the conductance-based model WITHOUT $K^+_{(Ca^{2+})}$ channel, which was absolutely necessary to induce a sustained spike inhibition in an isolated single neuron, indicating that the spike inhibition by TMS in the network was induced by mechanisms independent of the spike inhibition processes in an isolated single neuron mainly mediated by conductance incrase in $K^+_{(Ca^{2+})}$ channel. In addition, the temporal properties of the spike inhibition by both suprathreshold and subthreshold TMS observed in the network model agree with experimen-

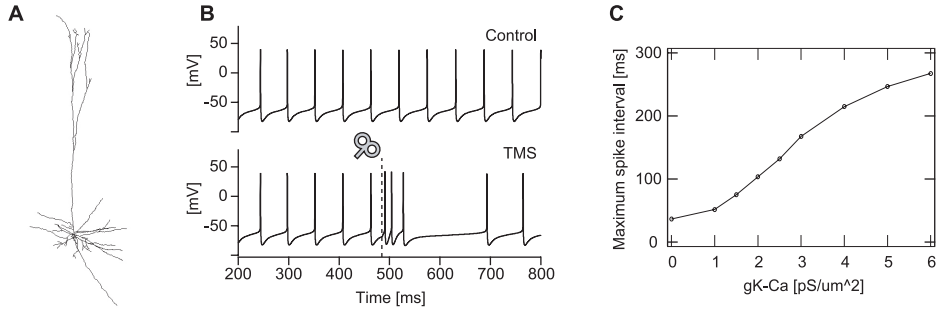

Fig. 3. A) Layer V pyramidal cell. B) The spike train could be suppressed by the perturbation, but C) the duration was strongly dependent on $K^{+}(Ca^{2+})$ (AHP) channel properties.

tal data of the occipital TMS [10]. These results suggest that each single neuron is not necessarily suppressed directly by TMS but the collapse of the excitatory-inhibitory balance and transsynaptic inhibitory interaction in the local network plays a critical role in TMS-induced suppresssion.

Acknowledgement

We greatly appreciate substantial support in programming by Takashi Shinozaki.

References

[1] Y. Kamitani, S. Shimojo, Manifestation of scotomas created by transcranial magnetic stimulation of human visual cortex., Nat Neurosci 2 (1999) 767–71.

[2] M. Inghilleri, A. Berardelli, G. Cruccu, M. Manfredi, Silent period evoked by transcranial stimulation of the human cortex and cervicomedullary junction., J Physiol 466 (1993) 521–34.

[3] A. Barker, R. Jalinous, I. Freeston, Non-invasive magnetic stimulation of human motor cortex., Lancet 1 (1985) 1106–7.

[4] S. Nagarajan, D. Durand, E. Warman, Effects of induced electric fields on finite neuronal structures: a simulation study., IEEE Trans Biomed Eng 40 (1993) 1175–88.

[5] Y. Kamitani, V. Bhalodi, Y. Kubota, S. Shimojo, A model of magnetic stimulation of neocortical neurons., Neurocomputing 38-40 (2001) 697–703.

[6] Y. Miyawaki, M. Okada, A network model of perceptual suppression induced by transcranial magnetic stimulation., Neural Comput 16 (2004) 309–31.

[7] Y. Miyawaki, M. Okada, Mechanism of neural interference by transcranial magnetic stimulation: network or single neuron?, Adv Neural Inf Process Syst 17.

[8] O. Shriki, D. Hansel, H. Sompolinsky, Rate models for conductance-based cortical neuronal networks., Neural Comput 15 (2003) 1809–41.

[9] Z. Mainen, T. Sejnowski, Influence of dendritic structure on firing pattern in model neocortical neurons., Nature 382 (1996) 363–6.

[10] P. Ray, K. Meador, C. Epstein, D. Loring, L. Day, Magnetic stimulation of visual cortex: factors influencing the perception of phosphenes., J Clin Neurophysiol 15 (1998) 351–7.